Anticipatory coadaptation of ankle stiffness and neural feedback for standing balance

Short title: Ankle stiffness and neural feedback in standing balance

Charlotte Le Mouel[1,2], Romain Brette[2]

1. corresponding author charlotte.lemouel@normale.fr, Max Planck Institute of Intelligent Systems, Stuttgart, Germany

2. Sorbonne Université, INSERM, CNRS, Institut de la Vision, 17 rue Moreau, F-75012 Paris, France.

I. Abstract

External perturbation forces may compromise standing balance. The nervous system can intervene only after a delay greater than 100 ms, during which the body falls freely. With ageing, neural feedback delays are prolonged, posing a critical threat to balance. We study a generic model of stabilisation with neural delays to understand how the organism should adapt to challenging balance conditions. The model suggests that ankle stiffness should be increased in anticipation of perturbations, for example by muscle co-contraction, so as to slow down body fall during the neural response delay. Increased ankle muscle co-contraction is indeed observed in young adults when standing in challenging balance conditions, and in elderly relative to young adults during normal stance. In parallel, the analysis of the model shows that increases in stiffness must be coordinated with decreases in spinal feedback gain, otherwise the feedback itself becomes destabilizing. Accordingly, a decrease in spinal feedback is observed in challenging conditions. These observations have been previously interpreted as indicating an increased reliance on cortical rather than spinal control of balance, despite the fact that cortical responses have a longer latency. Our analysis challenges this interpretation by showing that these observations are consistent with a functional coadaptation of spinal feedback gains to functional changes in stiffness.

II. Author summary

Being able to stand still can be difficult when faced with an unexpected push. It takes the nervous system more than a tenth of a second to respond to such a perturbation, and during this delay the body falls under the influence of its own weight. By co-contracting their ankle muscles in anticipation of a perturbation, subjects can increase their ankle stiffness, which slows down their fall during the neural delay. Young subjects indeed adopt this strategy when they need to remain particularly still (for example when they stand in front of a cliff). Elderly subjects adopt this strategy even during normal standing. We present a model of standing balance that shows that this postural strategy provides partial compensation for the increase in neural delays with ageing. According to our model, increasing ankle stiffness only improves balance if it is accompanied by a decrease in neural feedback. This provides a novel and functional interpretation for the decrease in spinal feedback observed during ageing, and observed in young subjects when they stand in challenging balance conditions.

III. Introduction

External perturbation forces may compromise standing balance (1). Current theories emphasise the role of the motor cortex in the feedback correction of unexpected perturbations (2,3). Indeed, the spinal feedback correction of perturbations is reduced when standing in challenging balance conditions (Figure 1.A), such as when standing facing a cliff (4), when standing on a narrow support (5) or simply when closing the eyes (6). The classical interpretation for this reduction in the spinal contribution to balance is that, in challenging conditions, the control of balance is delegated to supra-spinal structures, such as the cortex, which may allow for a more refined control than the spinal cord (3). Even in normal standing conditions, the spinal feedback correction of perturbations is reduced in elderly adults relative to young adults (Figure 1.B) (7–9), as well as delayed (10,11). The interpretation for this is likewise that elderly subjects rely more on cortical rather than spinal control of balance (2).

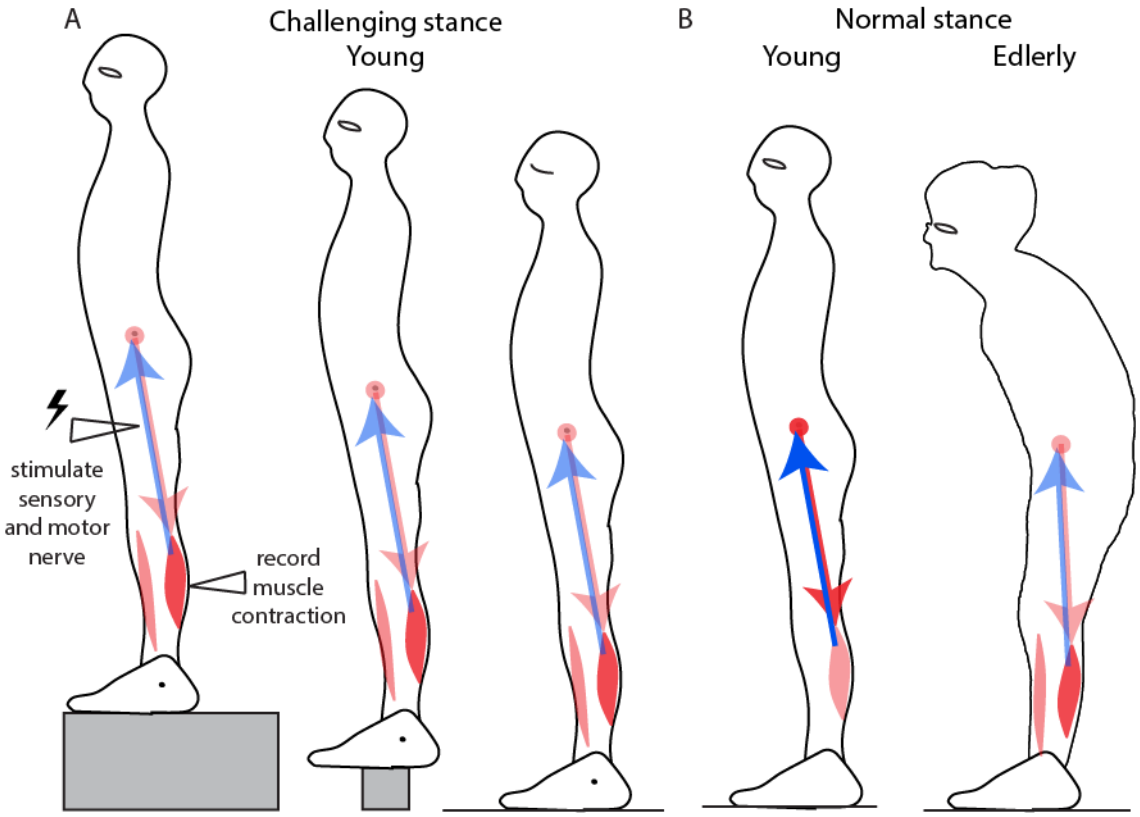

Figure 1 Ankle stiffness and spinal feedback. A. Decrease in soleus H-reflex in challenging balance conditions. Spinal feedback is probed by electrically stimulating the sensory fibres of a muscle and measuring the resulting change in muscle contraction, called the H-reflex. This H-reflex is larger in normal stance than when standing facing a cliff (left) (4), when standing on a narrow support (middle)(5) and standing with the eyes closed (right)(6). Co-contraction of antagonist ankle muscles is observed in each of these three cases. B. In normal stance the H-reflex is reduced in elderly (right) relative to young adults (left)(7–9). Co-contraction of antagonist ankle muscles during quiet standing is observed in elderly but not in young subjects (7,12).

The difficulty with this approach is that the neural feedback control of movement introduces delays. Thus, after a perturbation of stance, the earliest change in muscular contraction occurs with a delay of around 100 ms in young subjects (13,14). In elderly subjects, this is further delayed by 10 to 30 ms (13,14). The change in force due to this muscle contraction is only observed after an additional 40 ms (15). Responses involving the cortex have even longer delays than spinal feedback (16). It is well known from control theory that delays are critical when using sensory feedback to counteract external perturbations (17): thus, a system that is stabilized by feedback control may become unstable simply if the control delay increases. Relying on the cortex for feedback control would therefore increase instability. This may be particularly critical when standing in challenging balance conditions, or with age-related increases in neural delays.

During this neural response delay after a perturbation, the movement of the body is entirely determined by the body and environmental mechanical properties, such as stiffness, inertia and weight. Ankle stiffness can be actively increased through co-contraction of the ankle muscles (18). Young subjects co-contract the ankle muscles when standing in challenging balance conditions (5,6,19), and elderly subjects co-contract the ankle muscles even in normal standing conditions (Figure 1.B, right)(7,12). We present a model that demonstrates that increasing ankle stiffness in advance of a perturbation can improve robustness to perturbations, by reducing the amplification of perturbations during the neural feedback delay. However, this improves balance only if the increase in ankle stiffness is coordinated with a decrease in neural feedback, to prevent over-compensation. The decreased spinal feedback observed during normal standing in elderly subjects, and during standing in challenging balance conditions in young subjects, should therefore not be interpreted as the mark of a more cortical control of balance, but on the contrary as the sign that motor stabilisation is achieved through an increased reliance on ankle stiffness.

IV. Modelling results

After a perturbation of stance, the earliest change in muscular contraction occurs with a delay of around 100 ms in young subjects (13,14). The change in force due to this muscle contraction is only observed after an additional 40 ms (15). During this neural response delay $\tau_{delay} = 0.14\ s$, the body centre of mass is accelerated by gravity. We model the body mechanics using the single inverted pendulum model, which is widely used to model human stance in the sagittal plane (20,21). The ankle angle θ follows :

$$\ddot{\theta} = \frac{\theta}{\tau_{mech}^2}$$

$$\tau_{mech} = \sqrt{\frac{J}{mgLcos(\Theta_0) - k}}$$

The dynamics are thus governed by the mechanical time constant τ_{mech}, which captures the effects of the rotational inertia around the ankles J, ankle stiffness k and weight mg. Any increase in ankle stiffness k up to the critical ankle stiffness $K_{crit} = mgLcos(\Theta_0)$ increases the mechanical time constant of the body. Ankle stiffness thus slows down falling during the response delay (22). During this delay, perturbations are amplified by a factor $\exp(\frac{\tau_{delay}}{\tau_{mech}})$. This suggests that one strategy to improve immobility in challenging balance conditions may be to increase ankle stiffness so as to decrease the relative speed $S = \frac{\tau_{delay}}{\tau_{mech}}$. Increasing ankle stiffness may likewise help to compensate for an increase in feedback delay, by mitigating the increase in S.

We wish to determine how the neural feedback control of balance is affected in these two scenarios. For this, we first assume a simple model for the control of standing balance, and show that both strategies require a decrease in neural feedback. We then show that these results generalise to more complex neuro-mechanical models.

We first assume that balance is achieved through delayed feedback control of position and speed. Such a control strategy has previously suggested to model human balance in both the sagittal (21) and lateral (23) plane. This delayed proportional-derivative control has the form:

$$\ddot{\theta} = \frac{\theta}{\tau_{mech}^2} - p\theta\big(t - \tau_{delay}\big) - d\dot{\theta}(t - \tau_{delay})$$

1. Stability limits

For any combination of mechanical parameters (determining τ_{mech}) and neural response delay, there is a limited range of proportional gains p and derivative gains d that can stabilize the system (21). The equations of the stability boundaries are derived in the Supplementary (I) and provided in the Methods. They are plotted for increasing stiffness and neural delay in Figure 2.

With increasing ankle stiffness (i.e. increasing τ_{mech}, Figure 2.A), the minimal and maximal gains shift towards smaller values. Large values of feedback gains which are stable without ankle stiffness (Figure 2.A, black) become unstable with critical ankle stiffness (Figure 2.A, turquoise). Small values of feedback gains which are unstable without ankle stiffness become stable with critical ankle stiffness. This suggests that, if subjects increase ankle stiffness they may need to decrease their neural feedback.

With aging, there is in increase in feedback delay (13,14). According to our model, with increasing feedback delay (Figure 2.B), the range of stable feedback gain decreases. The maximal gains decrease sharply. If the subject increases ankle stiffness to compensate for the increasing delay (for example by keeping S constant, Figure 2.C), then the effects of increasing stiffness (Figure 2.A) and delay (Figure 2.B) combine. The proportional gains which can stabilise the system for $\tau_{delay} = 0.14\ s$ without ankle stiffness (Figure 2.C, black) are thus too large to stabilise the system after a doubling of the delay (Figure 2.C, yellow, $\tau_{delay} = 0.28\ s$, $k = 0.75\ K_{crit}$). This suggests that when subjects increase ankle stiffness to compensate for an increase in neural delay, they must decrease their neural feedback.

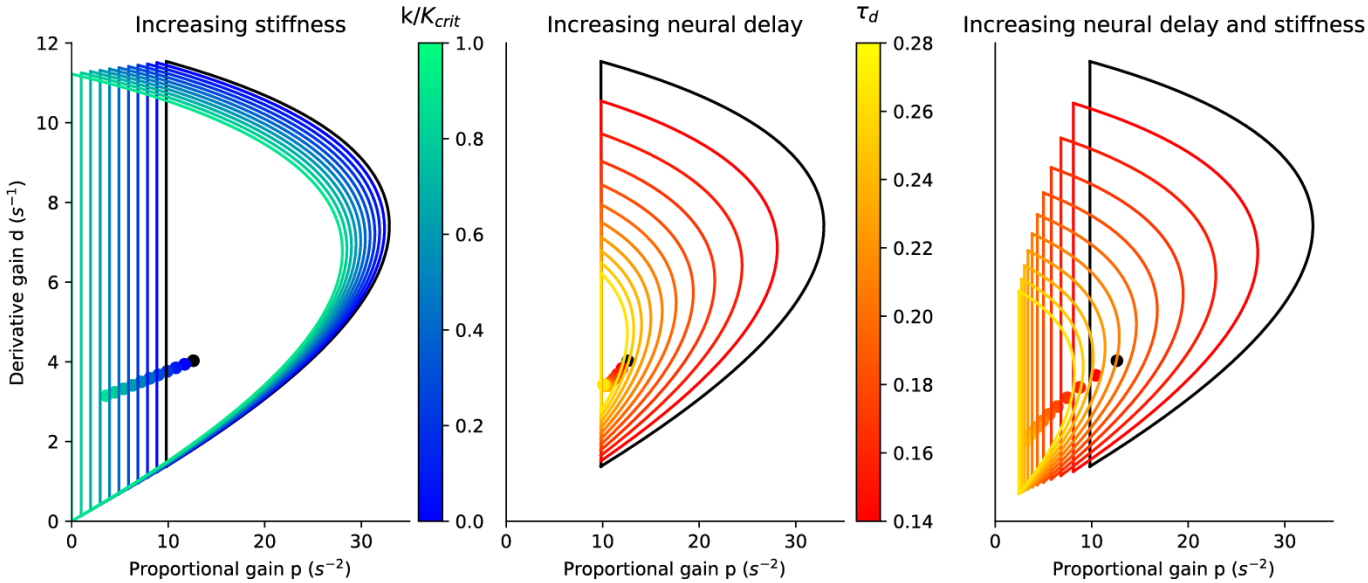

Figure 2 Stability limits of the proportional and derivative gains A. for stiffness increasing from 0 (black) to critical stiffness (turquoise) with a delay of 0.14 s; B. for a delay increasing from 0.14 s (black) to 0.28 s (yellow) without stiffness; C. for combined increases in delay and stiffness (maintaining a constant S), from a delay of 0.14 s with a stiffness of 0 (black) to a delay of 0.28 s with a stiffness of $0.75\ K_{crit}$ *(yellow). The critical feedback gains for each condition are indicated as dots. In the three panels, the black curves are identical and correspond to zero stiffness and a delay of 0.14 s.*

Within the range of stable feedback, large gain and low damping lead to oscillations, whereas low gain and large damping result in slow compensation for perturbations (as illustrated in the Methods). To determine how neural feedback is affected by an increase in stiffness or neural delay, we first determine the best combination of feedback gains and the resulting balance performance, for a given stiffness and delay.

2. Critical feedback gains

We assume that the best combination of feedback gains results in fast compensation of perturbations without oscillations. Subjects typically adopt such feedback gains when responding to lateral perturbations of stance (23). In second order systems governed by a characteristic polynomial $\lambda^2 + 2\zeta\,\omega_0\lambda + \omega_0^2$, for a given value of ω_0, the fastest compensation without oscillations occurs for the critical damping $\zeta = 1$. For such critical damping, the characteristic equation has a unique double root $-\omega_0$. If a perturbation brings the system away from its equilibrium position, then the system is returned to its initial position following the time-course $\exp(-\frac{t}{\tau_{balance}})$ where $\tau_{balance} = \frac{1}{\omega_0}$. Higher damping results in slower compensation for perturbations, whereas lower damping results in oscillations.

The characteristic equation of the system with delayed neural feedback is:

$$\lambda^2 - \frac{1}{\tau_{mech}^2} + d\lambda e^{-\tau_{delay}\lambda} + pe^{-\tau_{delay}\lambda} = 0$$

To determine the feedback gains which provide critical damping, we use a linear approximation to the delay introduced by Pade (24): $e^{\lambda} = \frac{1-\lambda/2}{1+\lambda/2}$. With this approximation, the characteristic equation becomes a third order polynomial, provided in the Methods. Then, we generalized the notion of critical damping to third order systems, considering that a system is critically damped when it has a unique triple negative root λ_0. The characteristic time to return to equilibrium is then $\tau_{balance} = -\frac{1}{\lambda_0}$. For each value of stiffness and delay, this procedure provided a unique value of $\tau_{balance}$ (Figure 3.A- C), and of the corresponding critical proportional gain p_{crit} (Figure 3.D-F) and derivative gain d_{crit} (Figure 3.G-I).

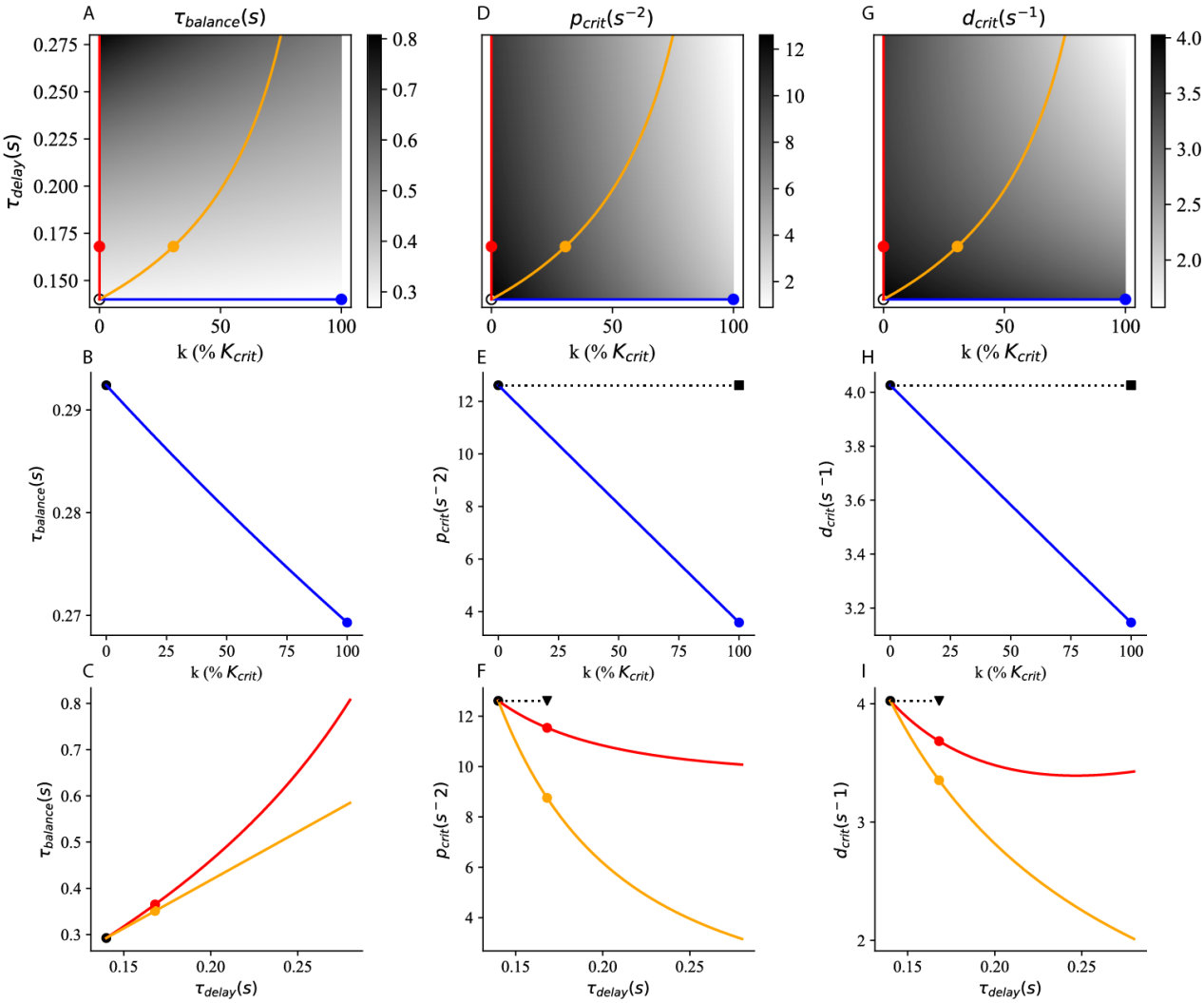

Figure 3 Critical feedback. The time to recover balance (A, B, C) and corresponding critical proportional (D, E, F) and derivative (G, H, I) gains are shown as a function of stiffness and neural delay. The strategy of increasing ankle stiffness with constant $\tau_{delay} = 0.14\ s$ is illustrated in blue. The effect of an increase in neural delay without ankle stiffness is illustrated in red. The strategy of increasing ankle stiffness to compensate for an increased delay (maintaining a constant S) is illustrated in orange. The values of the gains used in the simulations for Figures 4 and 5 are illustrated here as dots, squares and triangles.

In Figure 3.A, we show $\tau_{balance}$ as a function of ankle stiffness and neural delay. This corresponds to the time required to recover balance after a perturbation. Light shades of grey correspond to small values of $\tau_{balance}$ and therefore to good balance performance. Balance performance is best for large ankle stiffness and small neural delay (Figure 3.A, lower right corner). For a constant delay, $\tau_{balance}$ decreases with increasing ankle stiffness (Figure 3.A, B, blue curve). For constant ankle stiffness, $\tau_{balance}$ increases with increasing neural delay (Figure 3.A, C, red curve). When ankle stiffness and neural delay are jointly increased such that *S* remains constant, this mitigates the increase in $\tau_{balance}$ (Figure 3.A, C, orange curve).

The balance performance indicated by $\tau_{balance}$ is only achieved if the neural feedback gains provide critical damping. The critical proportional (Figure 3.D) and derivative (Figure 3.G) gains are largest for low ankle stiffness and neural delay (lower left corner). For a constant delay, the critical gains decrease with increasing ankle stiffness (Figure 3.D, E, G, H, blue curve). For constant ankle stiffness, the critical gains decrease with neural delay (Figure 3.D, F, G, I, red curve). When ankle stiffness and neural delay are jointly increased such that *S* remains constant, this amplifies the increase in critical gains (Figure 3. D, F, G, I, orange curve).

In the subsequent sections, we illustrate these results by simulating the response of the systems with the stiffness, delay and feedback gains indicated as circles, triangles and squares in Figure 3.

3. Improving stability in challenging balance conditions

In Figure 4 (left column), we show the response of the system with $\tau_{delay} = 0.14\ s$ to an external perturbation occurring at time 0, which causes an initial shift in ankle angle by an arbitrary distance 1. We first consider a system with critical stiffness and the corresponding critical feedback gains (blue dot in Figure 3). The initial perturbation causes an immediate increase in the torque of weight (Figure 4.A, left in grey). Since ankle stiffness perfectly compensates for the torque of weight, there is an immediate, equivalent and opposite increase in the ground reaction torque component due to stiffness (Figure 4.A, left in blue). Therefore, during the delay period (shaded in grey), the ankle angle (right panel) remains at a constant value. When the feedback control intervenes, a small increase in contraction (left panel, green) is sufficient to nudge the person back upright.

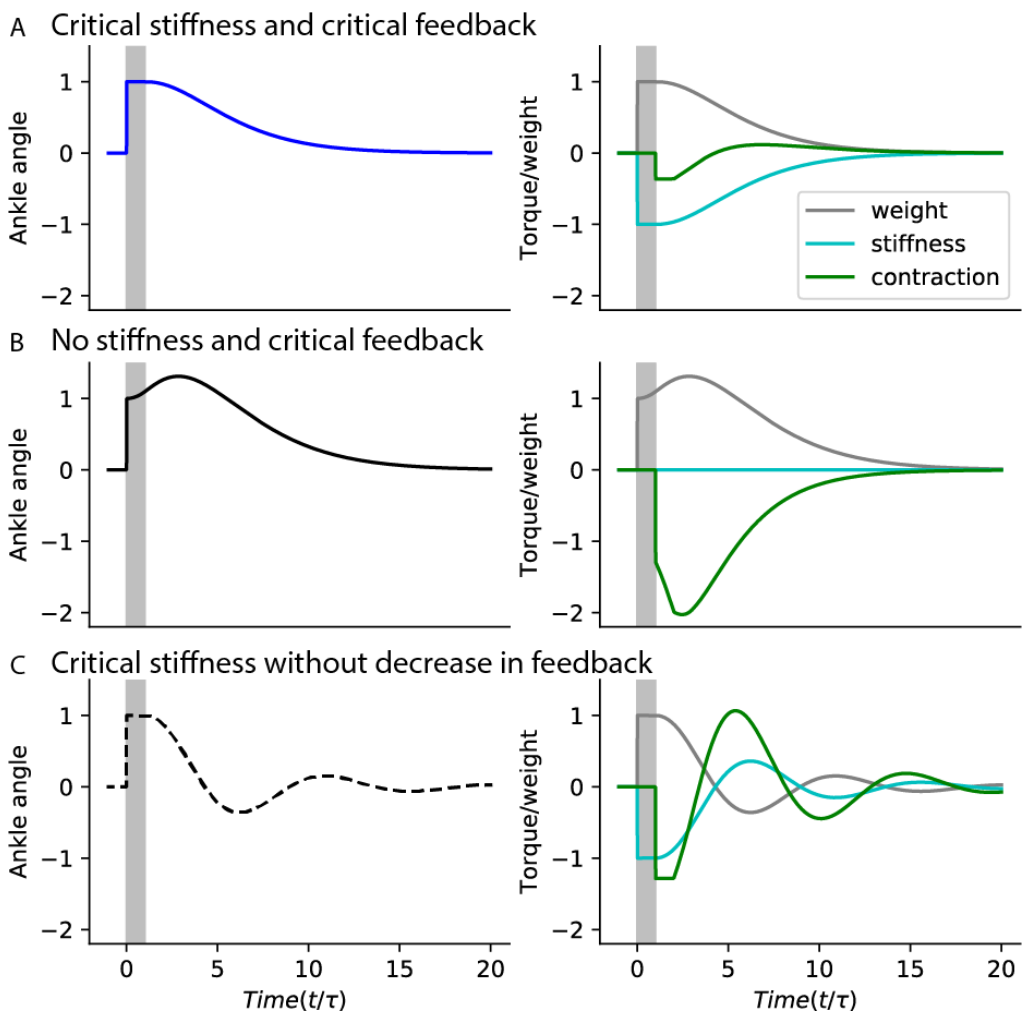

Figure 4 Increasing ankle stiffness. Simulated response to a perturbation in ankle angle of arbitrary amplitude 1. A. Response of the system with critical stiffness and critical feedback. B. Response of the system without stiffness, and with the corresponding critical feedback. C. Response of a system with critical stiffness, and with the same feedback controller as in B. The left panels show the time-course or the torque of weight (grey), and the components of the ground reaction torque due to stiffness (blue) and feedback contraction (green), normalised to weight. The right panels show the time-course of ankle angle. The response delay (between the perturbation and the first change in contraction) is shaded in grey.

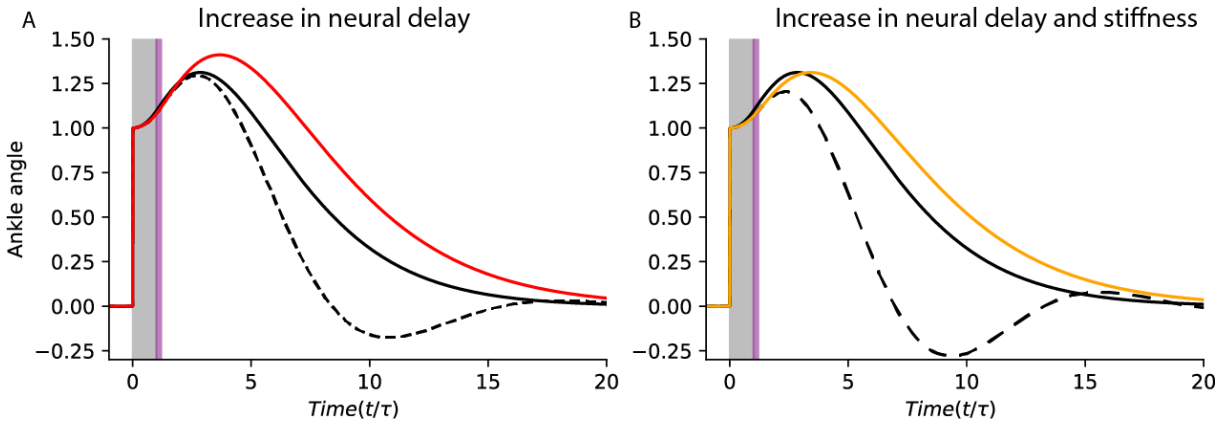

Figure 5 Compensation for increased feedback delays. A.B The simulated response to perturbation in ankle angle for the reference $\tau_{delay} = 0.14$ s (shaded gray bars) without ankle stiffness and with critical feedback is shown as a full black curve. A. Response of the system with a 20 % increase in delay (shaded purple bar) with critical feedback (red) and with the feedback appropriate for the reference delay (dashed black). B. Response of the system with a 20 % increase in delay (shaded purple bar) and a stiffness $k = 0.3\ K_{crit}$ with critical feedback (orange) and with the feedback appropriate for the reference delay (dashed black).

We then consider a system without ankle stiffness and with the corresponding critical feedback gains (black dot in Figure 3). The ground reaction torque component due to stiffness remains null (Figure 4.B, left in grey). During the delay period, the person therefore starts to fall, and picks up speed (right panel). When the feedback control intervenes, a large increase in contraction is therefore necessary to first slow down falling, then return the ankle angle to its initial position. The system without stiffness therefore requires larger feedback parameters.

If the system with critical stiffness is controlled with the feedback parameters appropriate for the system without stiffness (black square in Figure 3.E, H), then it is oscillatory (Figure 4.C). During the delay period, the person remains immobile. The large increase in contraction (left panel, green) then causes the ankle angle to overshoot its initial position, resulting in oscillations (right panel).

Increasing ankle stiffness therefore allows perturbations to be cancelled with less overshoot in ankle angle, and less change in muscle contraction, but it requires a coordinated decrease in feedback gains to prevent overshoot.

4. Compensating for increased feedback delays

With ageing, the ankle muscle responses to perturbations of stance are delayed by 10 to 30 % (13,14). To illustrate the effect of age-related increases in delay, we consider the intermediate value of a 20 % increase in delay, without ankle stiffness. If the person does not decrease their feedback gains (black triangle in Figure 3.F, I), the increase in delay results in oscillations (Figure 5.A, dashed black versus full black curve). If the person decreases their feedback gains to the critical value (red dot in Figure 3), they can cancel the perturbation without oscillations (Figure 5.A, red curve), but the overshoot is increased. To prevent this increase in overshoot, the appropriate strategy is to increase stiffness so as to maintain a constant S. If the person decreases their feedback gains to the critical value (orange dot in Figure 3), balance response (Figure 5.B, orange curve) is simply a scaled version of the reference balance response, stretched in time (Figure 5.B, full black curve). However, if the person does not decrease their feedback gains (black triangle in Figure 3.F, I), then the increase in stiffness does not improve balance (Figure 5.B, dashed black curve). Instead, it amplifies the oscillations due to the increase in feedback delay.

5. Generalisation to more complex neuromechanical models

Our modelling results show that, for a given neural delay, it is advantageous to increase the mechanical time constant to slow down body dynamics. Indeed, this decreases the amplification of perturbations during the response delay. In the sagittal plane, this can be achieved by stiffening the ankle. Moreover, our model predicts that when subjects adopt this strategy, they must additionally decrease their neural feedback gains to prevent

over-compensation. Additionally, our results show that following an increase in feedback delay, neural feedback gains must be decreased. These results generalise to more complex neuromechanical models.

The intrinsic damping properties of muscles are thought to be crucial for motor stabilization (25). We extend our model to include mechanical damping d_M such that:

$$\ddot{\theta} = \frac{\theta}{\tau_{mech}^2} - d_M\dot{\theta} - p\theta(t - \tau_{delay}) - d\dot{\theta}(t - \tau_{delay})$$

We apply our method for determining critical feedback to this extended model (see Methods), and we find that mechanical damping improves balance performance (decrease in $\tau_{balance}$ in Figure 6.A, D) and requires a larger proportional gain (Figure 6.B, E), and a smaller derivative gain (Figure 6.C, F). Our main result is however not affected: both increased stiffness (Figure 6.A-C) and neural delay (Figure 6.D-F) require a decrease in proportional and derivative gains.

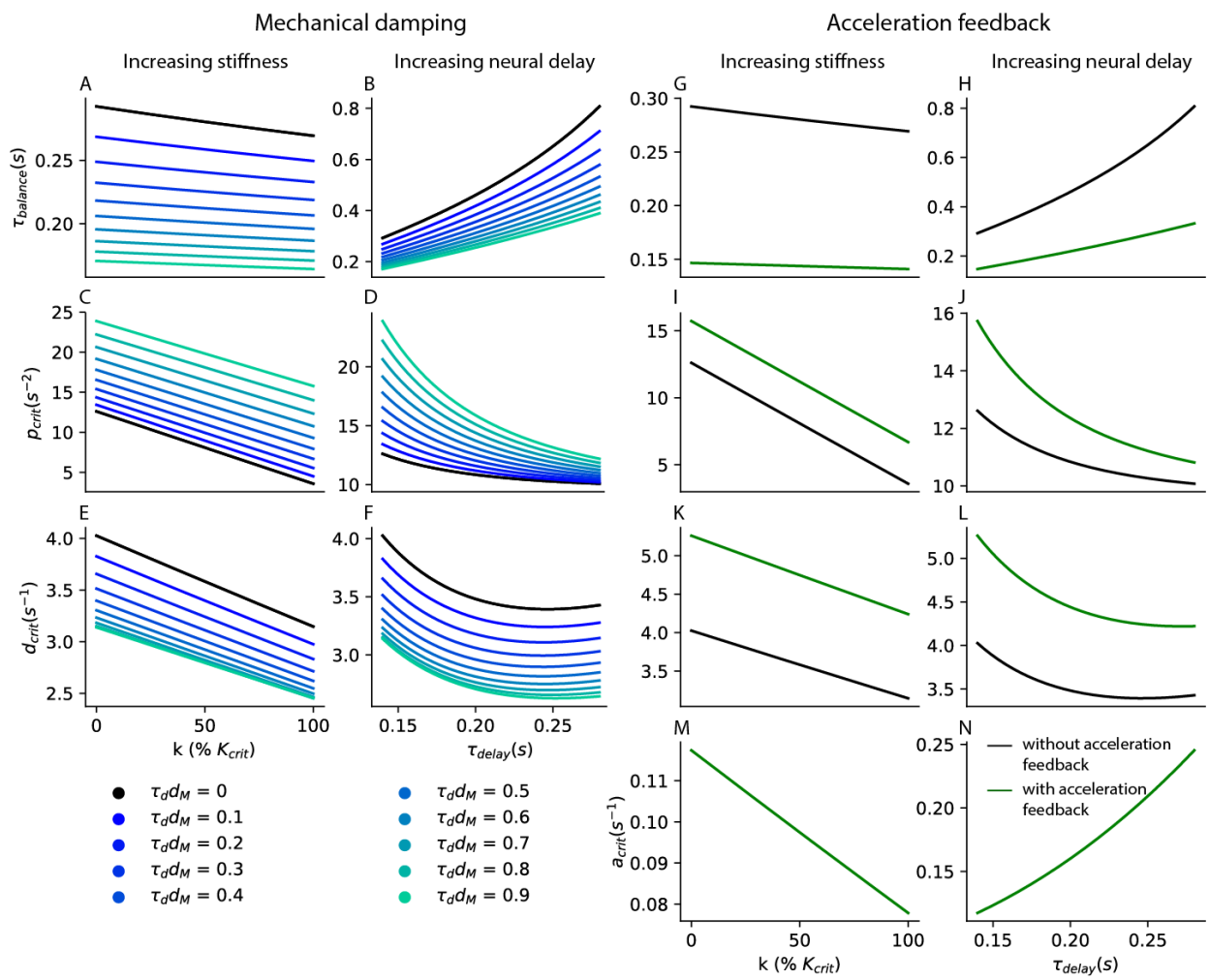

Figure 6 Generalisation to more complex neuromechanical models. A-F Mechanical damping d_M. The time to recover balance (A, B), critical proportional gain (C, D) and critical derivative gain (E, F) are shown for $\tau_{delay} = 0.14\ s$ and increasing ankle stiffness (A, C, E), and for null ankle stiffness and increasing neural delay (B, D, F). G-N Acceleration feedback a. The time to recover balance (G, H), critical proportional gain (I, J), critical derivative gain (K, L) and critical acceleration gain (M,N) are shown for $\tau_{delay} = 0.14\ s$ and increasing ankle stiffness (G, I, K, M), and for null ankle stiffness and increasing neural delay (H, J, L, N).

To fit the responses of human subjects to forwards and backwards perturbations of stance, Welch and Ting found that it was necessary to include acceleration feedback as well as proportional and derivative gains (20). We extend our model to include acceleration feedback A such that:

$$\ddot{\theta} = \frac{\theta}{\tau_{mech}^2} - p\theta\left(t - \tau_{delay}\right) - d\dot{\theta}(t - \tau_{delay}) - a\ddot{\theta}(t - \tau_{delay})$$

We apply our method for determining critical feedback to this extended model (see Methods), and we find that acceleration feedback improves balance performance (decrease in $\tau_{balance}$ in Figure 6.G, K) and requires a larger proportional gain (Figure 6.H, L), and derivative gain (Figure 6.I, N). Our main result is however not affected: both increased stiffness (Figure 6.A-C) and neural delay (Figure 6.D-F) require a decrease in proportional and derivative gains. The acceleration gain must be decreased for increasing ankle stiffness (Figure 6.M) and increased for increasing neural delay (Figure 6.N).

Finally, standing balance in the sagittal plane is better modelled by considering not only ankle angle but also hip angle (26) and knee angle (27). In the Methods, we show that our results also generalise to multi-dimensional systems.

V. Comparison to experiments

1. Improving stability in challenging balance conditions

When a subject is asked to stand in a situation in which it is particularly important not to move (Figure 1.A), an increase in ankle muscle co-contraction is observed, relative to normal stance. This occurs for example when standing facing a cliff (19), when standing on a narrow support (5) or simply when closing the eyes (6). Increased co-contraction increases ankle stiffness (18). According to our model, this decreases the amplification of perturbations during the response delay, thereby improving stability.

Such a strategy additionally requires a decrease in neural feedback. The spinal feedback gain can be probed experimentally using the H-reflex (28). This paradigm uses electrical stimulation of the calf muscle nerve to directly excite the sensory fibres embedded within the calf muscle (Figure 1, blue arrows), which are sensitive to the stretch and speed of stretch of the calf muscle, and therefore to both ankle angle and speed. In turn these sensory fibres directly excite the motor neurons of the ankle muscles, located in the spinal cord, which increase the contraction of the calf muscle (Figure 1, red arrow). The change in muscle contraction for a given electrical stimulation is called the H-reflex. In the challenging balance conditions for which increased ankle muscle co-contraction is observed, there is additionally a decrease in the spinal H-reflex (4–6). We suggest that this decrease in spinal feedback corresponds to the decrease in proportional and derivative critical feedback gains for increasing ankle stiffness, as derived in the Modelling results. Therefore, it is not indicative of an increased cortical control of posture, as commonly assumed, but is rather the hallmark of an increased reliance on body mechanics (namely ankle stiffness) for cancelling perturbations. In ballet dancers, which routinely practice balance in challenging situations, the spinal feedback gain is reduced compared to normal subjects, even in normal balancing conditions, such as when standing on flat, solid ground (29). We suggest that this may be due to a long term adjustment of the properties of the ankle muscles and tendons, leading to an increased ankle stiffness, such as may be observed in long-distance runners (30).

The human body comprises joints other than the ankle which are relevant for balance, such as the hip and knee joints (27). Our modelling results generalise to multi-dimensional systems and therefore predict that standing balance may also benefit from the stiffness of muscles acting at joints other than the ankle, if they slow down the amplification of perturbations during the response delay. This has indeed been shown by De Groote and colleagues, who asked human subjects to stand still despite external perturbations (31). They observed the resulting motion of the body during the time it takes for the nervous system to intervene, and attempted to reproduce this motion in simulations. They found that if muscle stiffness was not included in their simulations, then the simulated body fell much faster than the human subjects. Thus, human leg muscles are arranged in such a way that muscle stiffness slows down falling. This suggests that further increases in the stiffness of leg muscles (through

co-contraction) may be a useful strategy to further decrease falling speed. This would then require a decrease in neural feedback.

2. Compensation for increased feedback delays

With aging, there is an increase in the H-reflex latency of the ankle muscle soleus by 10 to 15 % (10,11). The response of ankle muscles to perturbations of stance is delayed by up 30 % (13,14). According to our model, elderly subjects may compensate for this increased neural delay through increased ankle stiffness. Indeed, elderly subjects have increased co-contraction of ankle muscles in quiet standing (7,12). In addition, the tissues around the ankle joint appear to be mechanically stiffer in elderly subjects: thus, when measured with relaxed muscles, the ankle stiffness of elderly subjects is higher than that of young subjects (32).

Our model additionally predicts that elderly subjects should decrease their feedback gains. Indeed, the soleus H-reflex has a reduced amplitude in the elderly compared to the young (7–9). Likewise, the stretch reflex in response to perturbations of stance has a reduced amplitude in elderly subjects (13). According to our model, this is appropriate to prevent oscillations.

VI. Discussion

1. Anticipatory co-adjustment of mechanical properties and feedback control for motor stabilisation

We have presented a generic model of stabilisation with neural response delays, which highlights the importance of the body mechanical properties for robustness to perturbations. We thus showed that the best stability is obtained when the body mechanical properties are adjusted so as to decrease the amplification of perturbations during the neural response delay. We additionally showed that this requires a coordinated decrease in feedback gains.

When standing on a narrow support, or in front of a cliff, it becomes particularly important to remain immobile. Our model predicts that the appropriate strategy is then to increase ankle stiffness and additionally decrease the neural feedback gains. We reviewed experimental evidence that young, healthy subjects can and do adopt this strategy. We therefore argue that the reduction in stretch reflex observed in these conditions is not the hallmark of increased cortical control, but on the contrary reflects an increased reliance on ankle stiffness.

During aging, the neural response delay to perturbations of stance increases. Our model predicts that the appropriate strategy is then to increase ankle stiffness and additionally decrease feedback gains. This is achieved in elderly adults through co-contraction, but also seems to rely on a long-term increase in stiffness of the tissues surrounding the ankle joint (32). We therefore argue that the reduction in stretch reflex observed in elderly subjects is not the hallmark of increased cortical control, but on the contrary reflects an increased reliance on ankle stiffness to compensate for neural delays.

2. Is stability maximised?

Ankle stiffness during stance is measured by imposing a rotation of the ankle and measuring the immediate change in ground reaction torque that ensues. Experimental measures vary from 40% to 90% of the critical stiffness (22,33–35). The observation that ankle stiffness is typically lower than the critical stiffness has given rise to a controversy on the relative importance of “passive” ankle stiffness and “active” neural feedback control for standing balance (36,37). Common to the two conflicting views is the assumption that ankle stiffness is a fixed mechanical property. These approaches thus fail to take into consideration the subjects’ ability to modulate ankle stiffness through ankle muscle co-contraction (18).

When standing in normal conditions, young subjects typically do not co-contract their ankle muscles; however, they are able to do so when it is particularly important to remain immobile (5,6,19). Likewise, during quiet standing, subjects continuously shift their position slightly over a range of around a centimetre; if however they are explicitly

instructed to remain as still as possible, then this range is divided by two (38). This suggests that in normal standing conditions, the standing posture is not adjusted to maximise stability. We have indeed recently developed a theory of postural control (39), according to which, during normal stance, posture is adjusted in view of mobility rather than immobility. This may induce subjects to adopt an ankle stiffness that is lower than the critical value. Indeed, maintaining a high ankle stiffness may prevent mobility, as it causes the ground reaction torque to immediately and mechanically cancel the torque of weight, whereas initiating a movement requires a net external torque to accelerate the movement (39). Thus, during normal standing in young adults, stability is not maintained at its maximal possible value, possibly due to trade-offs with both mobility and fatigue. However, young subjects can and do transiently increase their stability when this becomes important for motor performance, by adjusting the mechanical properties of their body in anticipation of the task.

When measured with relaxed muscles, ankle stiffness is larger in elderly relative to young subjects (32). Additionally, elderly subjects co-contract ankle muscles even during normal stance (7,12). This suggests a stronger emphasis on stability in elderly subjects than in young subjects. We suggest that this is a functional compensation for age-related increases in neural delays. However, since elderly subjects use co-contraction already for normal stance, they may be less able than young adults to transiently increase ankle stiffness in challenging balance conditions. Their overall balance may thus be affected. There is indeed an increasing incidence of falls with ageing (40). Moreover, the increase in stiffness of the passive tissues around the ankle joint suggests that elderly subjects may be less able than young subjects of transiently decreasing ankle stiffness at movement initiation. Their overall mobility may thus be affected. There is indeed an increasing incidence of mobility impairments with aging (41). Thus, although the age-related increase in ankle stiffness may allow elderly subjects to preserve stability in normal standing conditions, it may not be sufficient to ensure stability in challenging balance conditions, and it may come at the cost of a decrease in mobility.

VII. Methods

1. Mechanical model of stance: the single inverted pendulum

We consider the widely used model of human stance in the sagittal plane: the single inverted pendulum model presented in Figure 7 (20,21). When someone is standing on the ground, there are two external forces exerted on them: their weight and the ground reaction force (Figure 7). The point of application of the person's weight is called the centre of mass, noted CoM. The torque of weight around the person's ankles is thus $mg\mathrm{L}\sin(\Theta)$ (with m the person's mass, g gravity, L the CoM height and Θ the ankle angle). To understand the relative roles of body mechanical properties and feedback control in stabilisation, we decompose the ground reaction torque into a mechanical component $K(\Theta)$ due to ankle stiffness, which changes immediately upon a change in ankle angle, and a component C due to feedback muscle contraction with only changes after a delay τ_{delay} after a mechanical perturbation. The sum of the external torques affects the person's rotational momentum $J\dot{\Theta}$, where J is the rotational inertia around the ankles, according to the following equation:

$$J\ddot{\Theta} = m\,g\,L\sin(\Theta) - K(\Theta) - C$$

We consider that the person is initially at equilibrium at an angle Θ_0 with muscular contraction C_0, and linearize around this equilibrium, introducing θ, k, c such that:

$$\Theta = \Theta_0 + \theta$$
$$K(\Theta) = K(\Theta_0) + k\theta$$
$$C = C_0 + c$$

After linearization, the change in rotational momentum becomes:

$$J\ddot{\theta} = (mgLcos(\Theta_0) - k)\theta - c$$

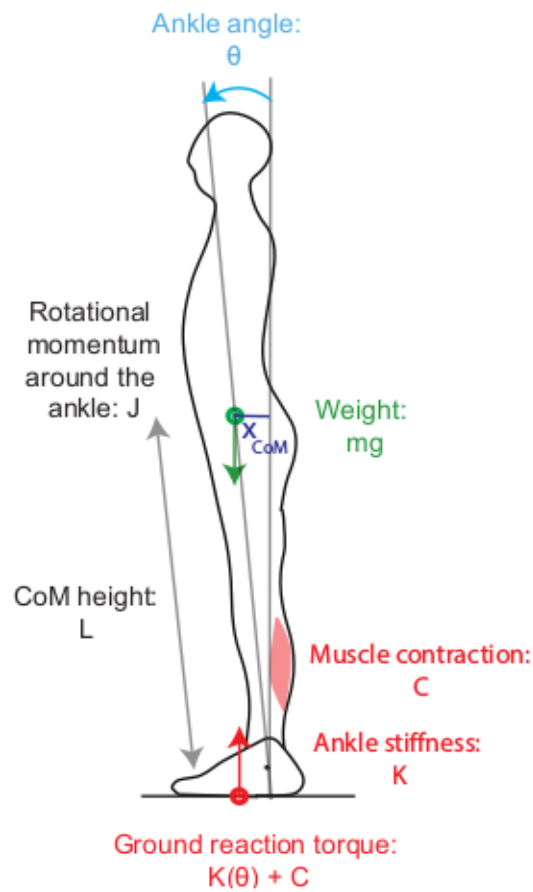

Figure 7 Single inverted pendulum model of stance. The external forces acting on the body are the weight (green arrow), whose torque around the ankle depends on ankle angle ϑ, and the ground reaction force (red arrow) whose torque depends on both ankle angle and muscle contraction.

The dynamics thus follows:

$$\ddot{\theta} = \frac{\theta}{\tau_{mech}^2} - \frac{c}{J}$$

$$\tau_{mech} = \sqrt{\frac{J}{mgLcos(\Theta_0) - k}}$$

The lower bound of τ_{mech} corresponds to $k = 0$. With mechanical parameters corresponding to human stance ($J \approx mL^2, L \approx 1\ m, \cos(\theta_0)\ \approx\ 1$), the minimal mechanical time constant is thus:

$$\tau_{m,0} = \sqrt{\frac{1}{9.81}} \approx 0.32\ s$$

For the neural feedback control, we consider a minimal time delay $\tau_{d,0} = 0.14\ s$.

Suppose an initial perturbation shifts the CoM position θ and speed $\dot{\theta}$ away from their initial equilibrium position to arbitrary values $\theta(t = 0) = \theta_0$, and $\dot{\theta}(t = 0) = \dot{\theta}_0$. During the neural response delay, the CoM position follows the time course:

$$\theta(t) = \frac{\theta_0 + \tau_{mech}\dot{\theta}_0}{2} e^{\frac{t}{\tau_{mech}}} + \frac{\theta_0 - \tau_{mech}\dot{\theta}_0}{2} e^{\frac{-t}{\tau_{mech}}}$$

Thus, by the time the nervous system intervenes at $t = \tau_{delay}$, the initial perturbation amplitude θ_0 has been amplified to the value $\theta(t = \tau_{delay}) = \theta_0 e^{\frac{\tau_{delay}}{\tau_{mech}}}$, and the initial perturbation speed has been amplified to $\dot{\theta}(t = \tau_{delay}) = \dot{\theta}_0 e^{\frac{\tau_{delay}}{\tau_{mech}}}$.

2. Stability analysis

We consider that the neural response follows a delayed proportional-derivative feedback controller, such that the dynamics of the system follows:

$$\ddot{\theta} = \frac{\theta}{\tau_{mech}^2} - p\theta(t - \tau_{delay}) - d\dot{\theta}(t - \tau_{delay})$$

The characteristic equation of the system is therefore:

$$\lambda^2 - \frac{1}{\tau_{mech}^2} + d\lambda e^{-\tau_{delay}\lambda} + pe^{-\tau_{delay}\lambda} = 0$$

The stability boundaries for this equation have been previously published (21). A derivation based on the Nyquist criterion is provided in S1.I. The boundary consists in two curves (Figure 8.A). The first is the line $p = \frac{1}{\tau_{mech}^2}$. The second is a curve parametrised by $\omega > 0$:

$$p(\omega) = \left(\omega^2 + \frac{1}{\tau_{mech}^2}\right)\cos(\omega\tau_{delay})$$
$$d(\omega) = \left(\omega^2 + \frac{1}{\tau_{mech}^2}\right)\frac{\sin(\omega\tau_{delay})}{\omega}$$

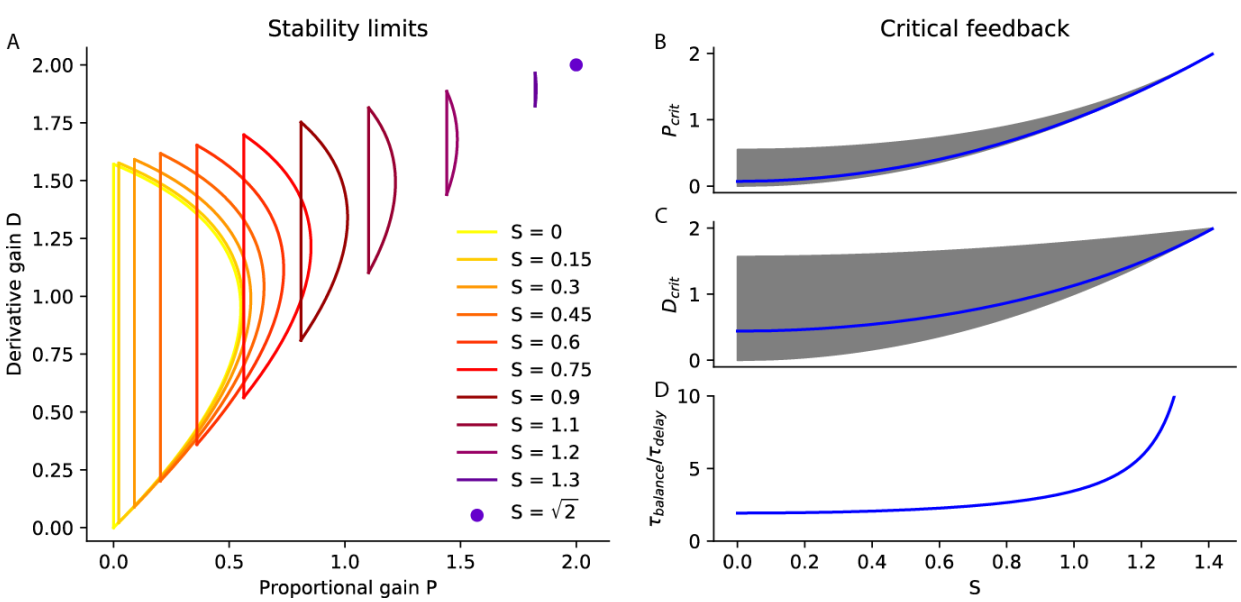

Figure 8 Delayed feedback control A. Stability limits. The range of stable normalised proportional and derivative gains (P and D) is plotted for different values of relative speed S ranging from S = 0 to the maximal S =$\sqrt{2}$. B-D Critical feedback. B. The critical proportional gain P_{crit} is plotted in blue as a function of S. The range of stable proportional gains is shaded in grey. C. The critical derivative gain D_{crit} is plotted in blue as a function of S. The range of stable derivative gains is shaded in grey. D. The time required to recover balance with critical feedback is plotted as a function of S.

We introduce the dimensionless variables: $x = \omega\tau_{delay}$, $P = p\tau_{delay}^2$, $D = d\tau_{delay}$, $S = \frac{\tau_{delay}}{\tau_{mech}}$. The second curve is then equivalent to the following curve, parametrised by $x > 0$:

$$P(x) = (x^2 + S^2)\cos(x)$$
$$D(x) = (x^2 + S^2)\frac{\sin(x)}{x}$$

In Figure 8.A, we show the range of feedback gains which can stabilise the system over a range of relative speeds S. For a given S, the stability limits for the proportional gain p scale with τ_{delay}^2 and those for the derivative gain d scale with τ_{delay}. We therefore plot the stability limits in terms of the dimensionless gains $P = p/\tau_{delay}^2$ and $D = d/\tau_{delay}$. For each value of S, there is a limited range of feedback gains (P, D) that can stabilize the system. This range is larger for slower values of S, suggesting slower systems are more robust to an inappropriate calibration of the feedback gains. Additionally, with increasing S, the range of stable gains shifts towards higher values. This shows that if the system speed S changes, then the feedback gains must be adjusted to maintain stability.

3. Critical feedback gains

The characteristic equation of the linearized inverted pendulum with delayed feedback control is:

$$\lambda^2 - \frac{1}{\tau_{mech}^2} + d\lambda e^{-\tau_{delay}\lambda} + pe^{-\tau_{delay}\lambda} = 0$$

We introduce the dimensionless variable $X = \tau_{delay}\lambda$. The roots of the characteristic equation are given by:

$$0 = \frac{1}{\tau_{delay}^2}\left(X^2 - \frac{\tau_{delay}^2}{\tau_{mech}^2} + d\tau_{delay}e^{-X} + p\tau_{delay}^2 e^{-X}\right) = \frac{1}{\tau_{delay}^2}(X^2 - S^2 + De^{-X} + Pe^{-X})$$

Critical damping is defined for second order systems governed by a characteristic equation of the form:

$$X^2 + 2\zeta\,\omega_0 X + \omega_0^2$$

To define critical damping for this system, we first introduce a rational function approximation for the delay, first proposed by Pade (24). With this approximation, the characteristic equation becomes a third order polynomial. We then generalize the notion of critical damping from second order to higher order polynomials.

a) Pade approximation

The first order Pade approximation of the delay is given by:

$$e^{-X} = \frac{e^{-X/2}}{e^{X/2}} \approx \frac{1 - X/2}{1 + X/2}$$

A dynamical systems interpretation of this approximation is provided in S1.II. With this approximation, the characteristic equation becomes:

$$X^2 - S^2 + Pe^{-X} + DXe^{-X} \approx (X^2 - S^2) + (P + DX)\frac{1 - X/2}{1 + X/2}$$
$$= \frac{1}{1 + \frac{X}{2}}\left((X^2 - S^2)\left(1 + \frac{X}{2}\right) + (P + DX)\left(1 - \frac{X}{2}\right)\right)$$
$$= \frac{1}{1 + \frac{X}{2}}\left(\frac{X^3}{2} + X^2\left(1 - \frac{P}{2}\right) + X\left(D - \frac{P}{2} - \frac{S^2}{2}\right) + P - S^2\right)$$

The roots of the approximate characteristic equation are thus the roots of:

$$X^3 + X^2(2 - D) + X(2D - P - S^2) + 2(P - S^2)$$

b) Generalisation of criticality to higher order polynomials

In second order systems governed by a characteristic equation $X^2 + 2\zeta\,\omega_0 X + \omega_0^2$, for a given value of ω_0, the fastest compensation without oscillations occurs for the critical damping $\zeta = 1$. For such critical damping, the

characteristic equation has a unique double root $-\omega_0$. Higher damping results in slower compensation for perturbations, whereas lower damping results in oscillations. We generalize the notion of 'critical damping', and consider that critical feedback in an nth order system corresponds to the system having a unique negative root $-\omega_0$ of order n.

c) Calculation

We therefore consider that our system is at criticality when is has a unique triple negative root $-\omega_0$. This requires: The coefficients of the characteristic equation must therefore correspond to the coefficients of the polynomial:

$$X^3 + X^2(2-D) + X(2D - P - S^2) + 2(P - S^2) = (X + \omega_0)^3 = X^3 + X^2 3\omega_0 + X\, 3{\omega_0}^2 + {\omega_0}^3$$

To find the critical feedback gains $\mathrm{P_{crit}}, \mathrm{D_{crit}}$ for a given relative speed S, we solve for $(\omega_0, \mathrm{P_{crit}}, \mathrm{D_{crit}})$ the system of equations:

$$0 = {\omega_0}^3 - 2(\mathrm{P_{crit}} - S^2) \qquad (1)$$
$$0 = 3{\omega_0}^2 - (2\mathrm{D_{crit}} - \mathrm{P_{crit}} - S^2) \qquad (2)$$
$$0 = 3\omega_0 - (2 - \mathrm{D_{crit}}) \qquad (3)$$

First we determine ω_0 as a function of S by removing (P, D) from the equations:
According to (3): $\mathrm{D_{crit}} = 2 - 3\omega_0$
According to (2): $\mathrm{P_{crit}} = 2D - S^2 - 3{\omega_0}^2 = 4 - 6\omega_0 - S^2 - 3\,{\omega_0}^2$
Replacing in (1):

$$0 = {\omega_0}^3 - 8 + 12\,\omega_0 + 2S^2 + 6{\omega_0}^2 + 2S = {\omega_0}^3 + 6{\omega_0}^2 + 12\,\omega_0 + 4S^2 - 8 = (\omega_0 + 2)^3 - 8 + 4S^2 - 8$$

Thus: $(\omega_0 + 2)^3 = 4(4 - S^2) > 0$
This equation admits one real positive solution for $(\omega_0 + 2)$, and two complex conjugate solutions. We take the real solution:

$$\omega_0 = -2 + (16 - 4S^2)^{\frac{1}{3}}$$

Replacing in (3): $\mathrm{D_{crit}} = 2 - 3\omega_0 = 8 - 3(16 - 4S^2)^{\frac{1}{3}}$
Replacing in (2): $\mathrm{P_{crit}} = 4 - 6\omega_0 - S^2 - 3\,{\omega_0}^2 = 4 + 12 - 6(16 - 4S^2)^{\frac{1}{3}} - S - 3(4 + (16 - 4S^2)^{\frac{2}{3}} - 4(16 - 4S^2)^{\frac{1}{3}})$

$$\mathrm{P_{crit}} = 4 - S^2 + 6(16 - 4S^2)^{\frac{1}{3}} - 3(16 - 4S^2)^{\frac{2}{3}}$$

d) Illustration

The response to a perturbation of the system with critical derivative gain and various values of the proportional gain is shown for $\tau_{delay} = 0.14\ s$ with critical stiffness (Figure 9.A) and without stiffness (Figure 9.B); and with a 20 % increase in delay, without stiffness (Figure 9.C). Proportional gains below the critical value (blue) result in slow compensation for perturbations. Proportional gains above the critical value (red) result in oscillations. These results are exacerbated without ankle stiffness and with increasing delay. This may even lead to instability.
The response to a perturbation of the system with critical proportional gain and various values of the derivative gain is shown for $\tau_{delay} = 0.14\ s$ with critical stiffness (Figure 9.D) and without stiffness (Figure 9.E); and with a 20 % increase in delay, without stiffness (Figure 9.F). Derivative gains below the critical value (blue) result in oscillations. Derivative gains above the critical value (red) result in slow compensation for perturbations. These results are exacerbated without ankle stiffness and with increasing delay.

The critical gains calculated thus provide the fastest compensation of perturbations without overshoot.

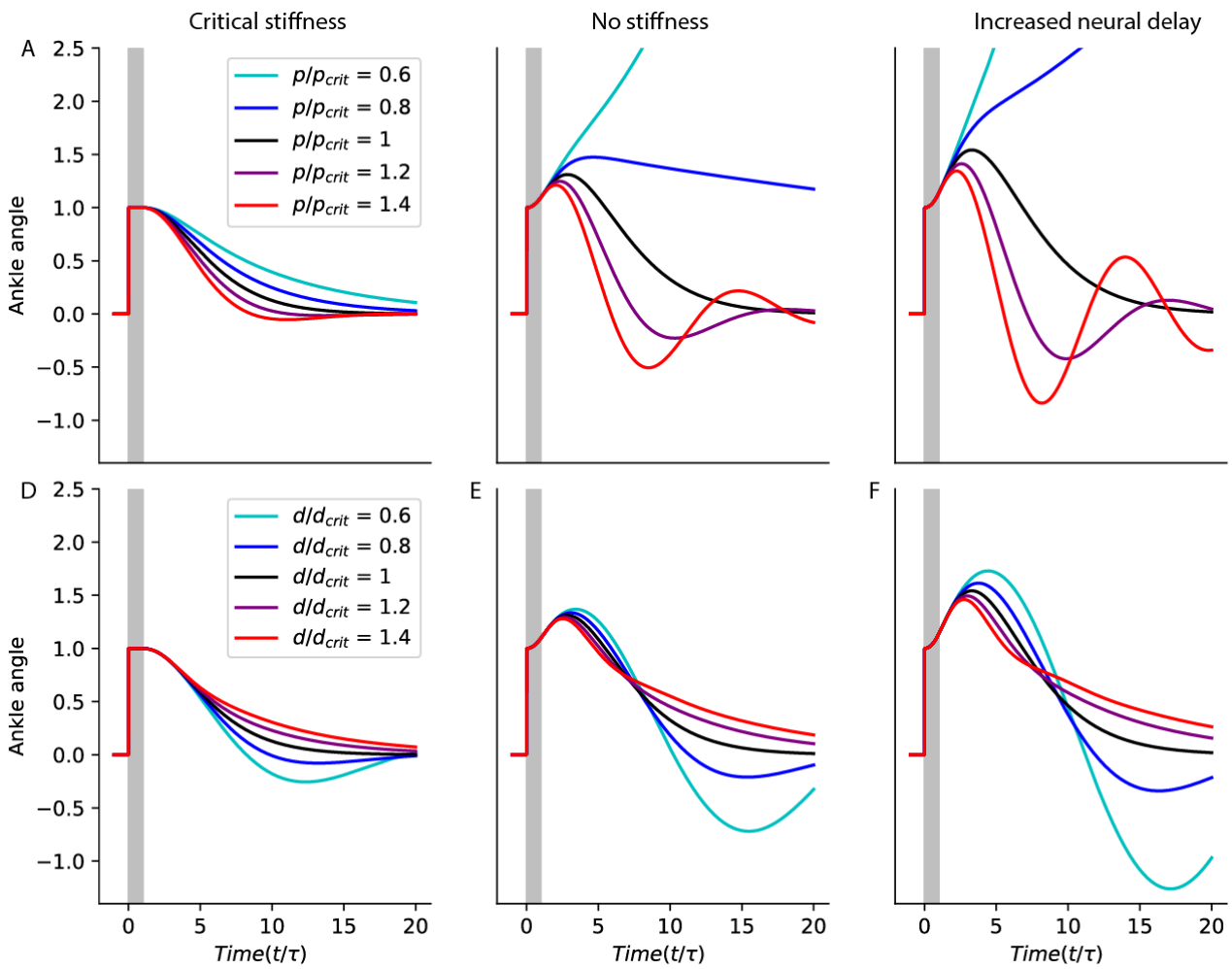

Figure 9 Illustration of critical feedback. Simulated response to a perturbation with critical derivative gain and various values of the proportional gain (A-C); and with critical proportional gain and various values of the derivative gain (D-E); for a system with $\tau_{delay} = 0.14$ s (A, B, D, E) and either critical stiffness (A, D) or no stiffness (B, E); and for a system with a 20% increase in delay and no stiffness (C, F).

e) Mechanical damping

We consider that the system has mechanical damping d_M such that:

$$\ddot{\theta} = \frac{\theta}{\tau_{mech}^2} - d_M\dot{\theta} - p\theta(t - \tau_{delay}) - d\dot{\theta}(t - \tau_{delay})$$

With the dimensionless damping $D_M = \tau_{delay} d_M$, the characteristic equation becomes:

$$X^2 + D_M X - S^2 + Pe^{-X} + DXe^{-X}$$

With the Pade approximation, its roots are those of:

$$(X^2 + D_M X - S^2)\left(1 + \frac{X}{2}\right) + (P + DX)\left(1 - \frac{X}{2}\right)$$
$$= \frac{1}{2}[X^3 + X^2(2 - D + D_M) + X(2D + 2D_M - P - S^2) + 2(P - S^2)]$$

For a given speed S and mechanical damping D_M, we numerically solve for $(\omega_0, \mathrm{P_{crit}}, \mathrm{D_{crit}})$ the system of equations:

$$0 = {\omega_0}^3 - 2(P - S^2)$$
$$0 = 3{\omega_0}^2 - (2D + 2D_M - P - S^2)$$
$$0 = 3\omega_0 - (2 - D + D_M)$$

The resulting time to recover balance and critical gains as a function of S are shown in Figure 10.A-C for increasing values of damping.

f) Acceleration feedback

We consider that the system has acceleration feedback A such that:

$$\ddot{\theta} = \frac{\theta}{\tau_{mech}^2} - p\theta\left(t - \tau_{delay}\right) - d\dot{\theta}(t - \tau_{delay}) - A\ddot{\theta}(t - \tau_{delay})$$

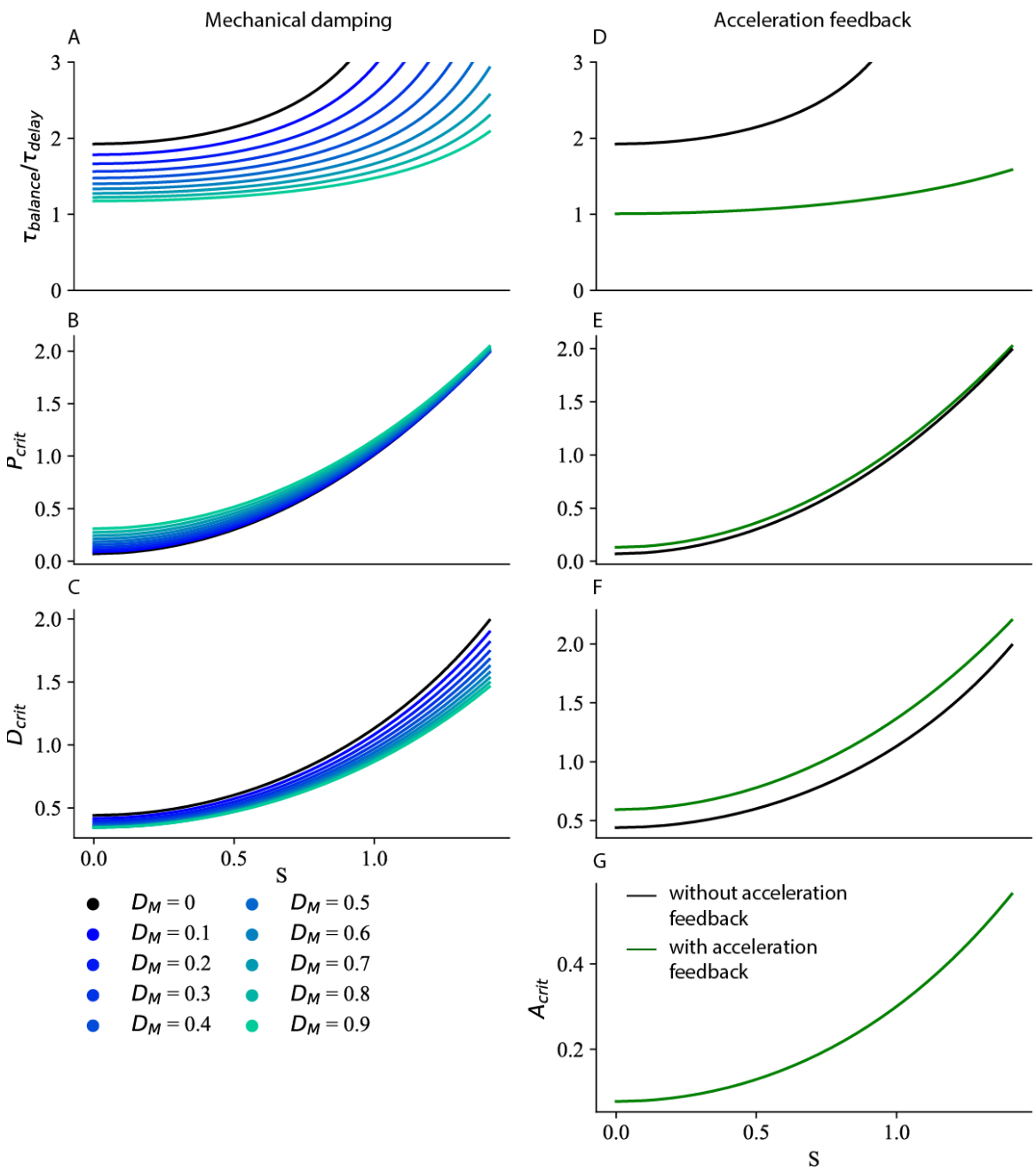

Figure 10 Mechanical damping and acceleration feedback. Time to recover balance (A, D), critical proportional gain (B, E), critical derivative gain (C, F) and critical acceleration gain (G) for increasing values of damping (A-C) and with acceleration feedback (D-G, green).

To calculate the critical feedback gains with acceleration feedback A, we must use the second order Pade approximation:

$$e^{-X} \approx \frac{X^2 - 4X + 8}{X^2 + 4X + 8}$$

With this approximation, the roots of the characteristic equation are given by:

$$(X^2 - S^2)(X^2 + 4X + 8) + (P + DX + AX^2)(X^2 - 4X + 8)$$
$$= X^4(1 + A) + X^3(4 + D - 4A) + X^2(8 - S^2 + P - 4D + 8A) + X(-4S^2 - 4P + 8D) + 8(P - S^2)$$

With critical feedback, this should have the same roots as:

$$X^4 + X^3(4\omega_0) + X^2(6\omega_0^2) + X(4\omega_0^3) + \omega_0^4$$

We numerically solve the system of equations:

$$0 = (1 + A)4\omega_0 - (4 + D - 4A)$$
$$0 = (1 + A)6\omega_0^2 - (8 - S^2 + P - 4D + 8A)$$
$$0 = (1 + A)4\omega_0^3 - (-4S^2 - 4P + 8D)$$
$$0 = (1 + A)\omega_0^4 - 8(P - S^2)$$

The resulting time to recover balance and critical gains as a function of S are shown in Figure 10.D-C in green.

g) Multi-dimensional systems

We consider an N-dimensional dynamical system with state $\boldsymbol{\theta}$ and delayed feedback control $\mathbf{C}$, whose dynamics are governed by:

$$\tau_{delay}{}^2 \frac{d^2}{dt^2}\begin{pmatrix}\theta_1\\ \cdots \\ \theta_N\end{pmatrix} = \begin{pmatrix} S_{1,1} & \cdots & S_{1,N} \\ \vdots & \ddots & \vdots \\ S_{N,1} & \cdots & S_{N,N}\end{pmatrix}\begin{pmatrix}\theta_1\\ \cdots \\ \theta_N\end{pmatrix} - \begin{pmatrix}C_1\\ \cdots \\ C_N\end{pmatrix}$$

$$\tau_{delay}{}^2 \ddot{\boldsymbol{\theta}} = \boldsymbol{S}\boldsymbol{\theta} - \mathbf{C}$$

We consider the generic case, in which the transpose $\boldsymbol{S}^T$ of the dynamics matrix $\boldsymbol{S}$ is diagonalizable, and introduce the basis set $(\boldsymbol{e_1}, \dots, \boldsymbol{e_N})$ of eigenvectors of $\boldsymbol{S}^T$ and their corresponding eigenvalues $(s_1, \dots, s_N)$, such that for every i:

$$\boldsymbol{S}^T \boldsymbol{e_i} = s_i \boldsymbol{e_i}$$

We use this basis set to perform a transformation of coordinates of the state $\boldsymbol{\theta}$ into $\boldsymbol{\alpha}$, such that, for every i, α_i is the dot product of the vectors $\boldsymbol{e_i}$ and $\boldsymbol{\theta}$:

$$\alpha_i = \boldsymbol{e_i}^T\, \boldsymbol{\theta}$$

Each component α_i follows the dynamical equation:

$$\tau_{delay}{}^2 \frac{d^2}{dt^2}\alpha_i = \boldsymbol{e_i}^T \boldsymbol{S}\boldsymbol{\theta} - \boldsymbol{e_i}^T \mathbf{C} = s_i \boldsymbol{e_i}\boldsymbol{\theta} - \boldsymbol{e_i}^T \mathbf{C} = \mathrm{s_i}\alpha_i - \boldsymbol{e_i}^T \mathbf{C}$$

The dynamics is thus decomposed into a set of N components, each of which follows a single-dimensional dynamics for which the analysis presented in the previous sections holds.
When considering a model of human stance with several joints (such as the ankle, knee and hip), the dynamics can be decomposed into such a set of components. Each of these components is a linear combination of the various angles, and its dynamics is governed by a mechanical time constant τ_i such that $s_i = \frac{\tau_{delay}^2}{\tau_i^2}$.

VIII. Funding

This work was supported by the Fondation pour la Recherche Médicale (grant number FDT20170437383) and the Agence Nationale de la Recherche (Axode ANR-14-CE13-0003).

IX. References

1. Le Mouel C, Tisserand R, Robert T, Brette R. Postural adjustments in anticipation of predictable perturbations allow elderly fallers to achieve a balance recovery performance equivalent to elderly nonfallers. conditionally accepted in Gait & posture, available on bioRxiv. 2018 Dec 26;506501.

2. Papegaaij S, Taube W, Baudry S, Otten E, Hortobágyi T. Aging causes a reorganization of cortical and spinal control of posture. Front Aging Neurosci. 2014;6.

3. Llewellyn M, Yang JF, Prochazka A. Human H-reflexes are smaller in difficult beam walking than in normal treadmill walking. Exp Brain Res. 1990;83(1):22–8.

4. Sibley KM, Carpenter MG, Perry JC, Frank JS. Effects of postural anxiety on the soleus H-reflex. Hum Mov Sci. 2007 Feb;26(1):103–12.

5. Trimble MH, Koceja DM. Effect of a reduced base of support in standing and balance training on the soleus H-reflex. Int J Neurosci. 2001 Jan;106(1–2):1–20.

6. Pinar S, Kitano K, Koceja DM. Role of vision and task complexity on soleus H-reflex gain. J Electromyogr Kinesiol. 2010 Apr;20(2):354–8.

7. Baudry S, Duchateau J. Age-related influence of vision and proprioception on Ia presynaptic inhibition in soleus muscle during upright stance. J Physiol (Lond). 2012 Nov 1;590(21):5541–54.

8. Koceja DM, Markus CA, Trimble MH. Postural modulation of the soleus H reflex in young and old subjects. Electroencephalogr Clin Neurophysiol. 1995 Dec;97(6):387–93.

9. Koceja DM, Mynark RG. Comparison of heteronymous monosynaptic Ia facilitation in young and elderly subjects in supine and standing positions. Int J Neurosci. 2000 Aug;103(1–4):1–17.

10. Sabbahi MA, Sedgwick EM. Age-related Changes in Monosynaptic Reflex Excitability. J Gerontol. 1982 Jan 1;37(1):24–32.

11. Scaglioni G, Narici MV, Maffiuletti NA, Pensini M, Martin A. Effect of ageing on the electrical and mechanical properties of human soleus motor units activated by the H reflex and M wave. The Journal of Physiology. 2004;548(2):649–61.

12. Nagai K, Yamada M, Uemura K, Yamada Y, Ichihashi N, Tsuboyama T. Differences in muscle coactivation during postural control between healthy older and young adults. Archives of Gerontology and Geriatrics. 2011 Nov 1;53(3):338–43.

13. Allum JHJ, Carpenter MG, Honegger F, Adkin AL, Bloem BR. Age-dependent variations in the directional sensitivity of balance corrections and compensatory arm movements in man. The Journal of Physiology. 2004;542(2):643–63.

14. Lin S-I, Woollacott MH. Postural Muscle Responses Following Changing Balance Threats in Young, Stable Older, and Unstable Older Adults. Journal of Motor Behavior. 2002 Mar 1;34(1):37–44.

15. Horak FB, Macpherson JM. Postural Orientation and Equilibrium. In: Comprehensive Physiology. American Cancer Society; 2011. p. 255–92.

16. Pruszynski JA, Scott SH. Optimal feedback control and the long-latency stretch response. Exp Brain Res. 2012 May;218(3):341–59.

17. Aström KJ, Murray RM. Feedback Systems: An Introduction for Scientists and Engineers. Princeton University Press; 2010.

18. Nielsen J, Sinkjær T, Toft E, Kagamihara Y. Segmental reflexes and ankle joint stiffness during co-contraction of antagonistic ankle muscles in man. Exp Brain Res. 1994 Dec 1;102(2):350–8.

19. Carpenter MG, Frank JS, Silcher CP, Peysar GW. The influence of postural threat on the control of upright stance. Exp Brain Res. 2001 May;138(2):210–8.

20. Welch TDJ, Ting LH. A feedback model reproduces muscle activity during human postural responses to support-surface translations. J Neurophysiol. 2008 Feb;99(2):1032–8.

21. Stepan Gabor. Delay effects in the human sensory system during balancing. Philosophical Transactions of the Royal Society A: Mathematical, Physical and Engineering Sciences. 2009 Mar 28;367(1891):1195–212.

22. Loram ID, Maganaris CN, Lakie M. The passive, human calf muscles in relation to standing: the non-linear decrease from short range to long range stiffness. J Physiol (Lond). 2007 Oct 15;584(Pt 2):661–75.

23. Bingham JT, Choi JT, Ting LH. Stability in a frontal plane model of balance requires coupled changes to postural configuration and neural feedback control. Journal of Neurophysiology. 2011 May 4;106(1):437–48.

24. Hanta V, Procházka A. Rational Approximation of Time Delay. 2009.

25. Haeufle DFB, Grimmer S, Kalveram K-T, Seyfarth A. Integration of intrinsic muscle properties, feed-forward and feedback signals for generating and stabilizing hopping. J R Soc Interface. 2012 Jul 7;9(72):1458–69.

26. Colobert B, Crétual A, Allard P, Delamarche P. Force-plate based computation of ankle and hip strategies from double-inverted pendulum model. Clinical Biomechanics. 2006 May 1;21(4):427–34.

27. Günther M, Wagner H. Dynamics of quiet human stance: computer simulations of a triple inverted pendulum model. Computer Methods in Biomechanics and Biomedical Engineering. 2016 Jun 10;19(8):819–34.

28. Knikou M. The H-reflex as a probe: Pathways and pitfalls. Journal of Neuroscience Methods. 2008 Jun 15;171(1):1–12.

29. Mynark RG, Koceja DM. Comparison of soleus H-reflex gain from prone to standing in dancers and controls. Electroencephalogr Clin Neurophysiol. 1997 Apr;105(2):135–40.

30. Kubo K, Miyazaki D, Yamada K, Yata H, Shimoju S, Tsunoda N. Passive and active muscle stiffness in plantar flexors of long distance runners. J Biomech. 2015 Jul 16;48(10):1937–43.

31. De Groote F, Allen JL, Ting LH. Contribution of muscle short-range stiffness to initial changes in joint kinetics and kinematics during perturbations to standing balance: A simulation study. Journal of Biomechanics. 2017 Apr 11;55:71–7.

32. Vandervoort AA, Chesworth BM, Cunningham DA, Paterson DH, Rechnitzer PA, Koval JJ. Age and Sex Effects on Mobility of the Human Ankle. J Gerontol. 1992 Jan 1;47(1):M17–21.

33. Casadio M, Morasso PG, Sanguineti V. Direct measurement of ankle stiffness during quiet standing: implications for control modelling and clinical application. Gait & Posture. 2005 Jun 1;21(4):410–24.

34. Lang CB, Kearney RE. Modulation of ankle stiffness during postural sway. In: 2014 36th Annual International Conference of the IEEE Engineering in Medicine and Biology Society. 2014. p. 4062–5.

35. Vlutters M, Boonstra TA, Schouten AC, van der Kooij H. Direct measurement of the intrinsic ankle stiffness during standing. Journal of Biomechanics. 2015 May 1;48(7):1258–63.

36. Morasso PG, Sanguineti V. Ankle Muscle Stiffness Alone Cannot Stabilize Balance During Quiet Standing. Journal of Neurophysiology. 2002 Oct 1;88(4):2157–62.

37. Winter DA, Patla AE, Prince F, Ishac M, Gielo-Perczak K. Stiffness control of balance in quiet standing. J Neurophysiol. 1998 Sep;80(3):1211–21.

38. Loram ID, Kelly SM, Lakie M. Human balancing of an inverted pendulum: is sway size controlled by ankle impedance? J Physiol (Lond). 2001 May 1;532(Pt 3):879–91.

39. Le Mouel C, Brette R. Mobility as the Purpose of Postural Control. Front Comput Neurosci. 2017;11:67.

40. Masud T, Morris RO. Epidemiology of falls. Age Ageing. 2001 Nov;30 Suppl 4:3–7.

41. Holmes J, Powell-Griner E, Lethbridge-Cejku M, Heyman K. Aging differently: Physical limitations among adults aged 50 years and over: United States, 2001-2007. NCHS Data Brief. 2009 Jul;(20):1–8.